[16] Ligand–Protein Interactions via Nuclear Magnetic Resonance of Quadrupolar Nuclei

By CHARLES R. SANDERS II and MING-DAW TSAI

Introduction

A significant number of biologically relevant elements have isotopes that possess nuclear magnetic spin quantum numbers greater than $\frac{1}{2}$ and thereby possess nuclear quadrupole moments. This results in the powerful quadrupolar relaxation mechanism that normally dominates the relaxation and, therefore, the line shapes and widths of the NMR peaks observed from such nuclei. To a certain extent, quadrupolar NMR (QNMR) is advantageous because only a single relaxation mechanism is effectively operative. However, because of theoretical and experimental difficulties, QNMR is an underdeveloped and underutilized technique in the study of biological systems, particularly in enzymology. Keniry ([19], Vol. 176, this series) deals with ^{2}H NMR of ^{2}H-labeled proteins, where the useful information extracted regards the local dynamics of amino acid side chains. This chapter presents the use of QNMR to study ligand–protein or substrate–enzyme interactions. In addition to the possible determination of stoichiometry, binding constants, and exchange rates, QNMR can be a particularly effective method in the study of the motional dynamics (through determination of τ_c, the effective correlation time) and the electrical environment (through χ, the quadrupolar coupling constant) of bound ligands. The term QNMR should not be confused with a related physical technique: nuclear quadrupole resonance. Because the studies we are concerned with usually involve motion that is isotropic on the NMR time scale, we are technically concerned with high-resolution (HR) NMR. However, because QNMR lines tend to be rather broad, the practical study of quadrupolar species tends to involve a mixture of HR and "broad-line" NMR techniques.

Some aspects of QNMR have been discussed in a number of recent reviews.[1-6] This chapter emphasizes practical aspects and is written spe-

[1] P. Laszlo (ed.), "NMR of Newly Accessible Nuclei: Chemical and Biological Applications," Vols. 1 and 2. Academic Press, New York, 1983.
[2] S. Forsén, T. Drakenberg, and H. Wennerström, *Q. Rev. Biophys.* **19**, 83 (1987).
[3] S. Forsén and B. Lindman, *Methods Biochem. Anal.* **27**, 289 (1981).
[4] J. B. Lambert and F. G. Riddell (eds.), *NATO Adv. Study Ser., Ser. C* **103** (1983).
[5] M. Minelli, J. H. Enemark, R. T. C. Brownlee, M. J. O'Connor, and A. G. Webb, *Coord. Chem. Rev.* **68**, 169 (1985).
[6] H. Mantsch, H. Saito, and I. P. Smith, *Prog. NMR Spectrosc.* **11**, 211 (1977).

Copyright © 1989 by Academic Press, Inc.
All rights of reproduction in any form reserved.

cifically for biochemists with a general knowledge of HR NMR but without previous experience in QNMR.

Fundamental Considerations in Experimental Design

Sensitivity

Three factors contribute to the sensitivity problem in QNMR. (1) As shown in Table I, the intrinsic sensitivity of most quadrupolar nuclei is much lower than that for ^1H. Furthermore, many nuclei have low natural abundance. (2) Linewidths of quadrupolar species are often broad and the amount of sample is often limited in biochemically relevant studies. (3) Because T_1 and T_2 are usually very short for quadrupolar nuclei, the loss of signal during the "preacquisition delay" (DE; see Experimental Techniques) becomes a detrimental factor to sensitivity. On the other hand, short T_1 and T_2 allow rapid acquisition, and it is sometimes possible to collect as many as 10^6 scans within 24 hr.

To attain a rough estimate of the limit of detection of a sample and spectrometer system, it is often advisable to prepare a standard sample of the free ligand (or a structurally similar compound) at the same concentration as that to be used in the experiment of interest. If a signal can be

TABLE I
PARAMETERS FOR SELECTED QUADRUPOLAR NUCLEI OF BIOLOGICAL INTEREST

Nucleus	I	Natural abundance (%)	Sensitivity (relative to ^1H)	Q (10^{-28} m^2)	Typical χ range (MHz)	Typical δ range (ppm)	Typical linewidth for τ_c = 0.1 nsec (Hz)
^6Li[a]	1	7.4	0.01	0.0007	<0.01	5	0.01
^7Li	3/2	92.6	0.29	−0.03	0.015–0.15	5	0.7
^{14}N	1	99.6	0.001	0.016	1–5	200	4,200
^{17}O	5/2	0.037	0.03	−0.026	1–15	700	3,000
^2H[b]	1	0.015	0.01	0.0027	0.16–0.22	10	19
^{23}Na	3/2	100	0.1	0.14	0.2–2	20	125
^{25}Mg	5/2	10	0.003	0.22	1–4	—	120
^{33}S	3/2	0.76	0.002	−0.064	0.5–15	600	7,000
^{35}Cl	3/2	75	0.005	−0.079	1–4	700	500
^{39}K	3/2	93	0.0005	0.11	—	30	—
^{43}Ca	7/2	0.15	0.006	−0.065	0.5–4	70	29
^{59}Co	7/2	100	0.28	0.40	2–80	18,000	20,000

[a] Quadrupolar relaxation generally does not dominate in ^6Li NMR.
[b] Despite low Q, quadrupolar relaxation dominates due to nonspherical symmetry.

detected, the viscosity can be varied using glycerol and decreasing temperature to broaden the signal, until it reaches the limit of detection.

Chemical Shifts and Spin–Spin Coupling

As exemplified in Table I, the chemical shift range of each nucleus is variable. Observed chemical shifts are, of course, potential sources of information. However, the resolution of multiple signals is a problem when chemical shift differences do not exceed linewidths. This factor tends to limit the number of species observable in a single sample.

Because lines are often broad in QNMR, spin–spin coupling is frequently unobservable. Nevertheless, coupling constants are sometimes large enough to affect the spectra through broadening[7,8] or splitting[8,9] and must then be taken into account in determining line shape or linewidth ($\Delta\nu_{1/2}$).

Relaxation in the Absence of Chemical Exchange

Longitudinal (T_1) and transverse (T_2) relaxation for $I > \frac{1}{2}$ nuclei in the absence of chemical exchange is usually dominated by quadrupole-induced relaxation. Transverse relaxation largely dictates the shape and width of NMR peaks.

Quadrupolar relaxation properties are generally classified in two defined regions: extreme narrowing (where $\omega_0^2\tau_c^2 \ll 1$) or nonextreme narrowing (where $\omega_0^2\tau_c^2 \gtrsim 1$), where ω_0 is the angular Larmor frequency of the nuclei.

The rotational correlation time τ_c is related to the molecular tumbling rate: the faster the motion, the smaller the τ_c. This parameter can be roughly estimated for use in predicting the narrowing region using the Stokes–Einstein–Debye equation[10]:

$$\tau_c = 4\pi\eta r^3/3kT \tag{1}$$

where k is Boltzmann's constant, T is in degrees Kelvin. η is solution viscosity (~1 cP for H_2O at 20°), and r is the radius of the molecule. Yguerabide *et al.*[11] listed the τ_c values calculated from Eq. (1) and determined experimentally for a number of proteins of varying molecular weight. The τ_c value of a protein represents only the upper limit of the τ_c of the bound ligand, because the bound ligand is likely to possess some internal rotational freedom.

[7] S.-L. Huang and M.-D. Tsai, *Biochemistry* **21**, 951 (1982).
[8] D. Sammons, P. A. Frey, K. Bruzik, and M.-D. Tsai, *J. Am. Chem. Soc.* **105**, 5455 (1983).
[9] J. A. Gerlt, P. C. Demou, and S. Mehdi, *J. Am. Chem. Soc.* **104**, 2848 (1982).
[10] W. Egan, *J. Am. Chem. Soc.* **98**, 4091 (1976).
[11] J. Yguerabide, H. F. Epstein, and L. Stryer, *J. Mol. Biol.* **51**, 573 (1970).

Relaxation in the Extreme Narrowing Limit. In this region transverse and longitudinal relaxations are both monoexponential decays characterized by single relaxation times related to the observed linewidth as follows:

$$\Delta\nu_{1/2} = \frac{1}{\pi T_2} = \frac{1}{\pi T_1} = \frac{3\pi}{10}\frac{2I+3}{I^2(2I-1)}\left(1+\frac{\eta^2}{3}\right)\left(\frac{e^2q_{zz}Q}{h}\right)^2\tau_c \qquad (2)$$

The proportionality between τ_c and linewidth $\Delta\nu_{1/2}$ is evident: slow-moving species produce large linewidths. Equation (2) has been widely used to deduce τ_c from the observed linewidth in QNMR.

The term $(e^2q_{zz}Q/h)$ is the quadrupolar coupling constant (χ) that describes the strength of the interaction of the quadrupole moment with its electric environment. This interaction is the physical basis for the quadrupolar relaxation mechanism. Q is the intrinsic quadrupole moment of the nucleus, e is the charge of the electron, and q_{zz} is the largest component of the electric field gradient interacting with Q and vanishes when electric symmetry around the nucleus becomes very high (e.g., T_d or O_h groups).

Table I shows that Q varies considerably from nucleus to nucleus. In the case of ^{6}Li and ^{7}Li, χ^2 can be so small that other relaxation mechanisms can actually compete, while for high-Q nuclei χ^2 is often so large that peaks become very broad, even for free ligands (unless q_{zz} is very low due to high symmetry).

The asymmetry parameter η varies from 0 to 1 and describes the deviation of the electric field gradient from axial symmetry ($\eta = 0$ for axial symmetry). Because even in the rare instance that $\eta = 1$ the term $1 + \eta^2/3$ is only 1.33, the asymmetry parameter can usually be neglected.

Relaxation Outside of Extreme Narrowing. As molecular motion becomes slower and $\omega_0^2\tau_c^2$ approaches or exceeds 1, Eq. (2) no longer holds. T_2 and T_1 become nonequivalent: T_2 continues to get smaller (with corresponding broader linewidths), while T_1 starts to get larger. In the case of $I = 1$, nuclei lineshapes remain Lorentzian and T_1 and T_2 are described by Eqs. (3) and (4), respectively[12,13] [which reduce to Eq. (2) when $\omega_0^2\tau_c^2 \ll 1$]:

$$\frac{1}{T_1} = \frac{3\pi^2}{100}\frac{2I+3}{I^2(2I-1)}\chi^2\left(1+\frac{\eta^2}{3}\right)\left(\frac{2\tau_c}{1+\omega_0^2\tau_c^2}+\frac{8\tau_c}{1+4\omega_0^2\tau_c^2}\right) \qquad (3)$$

[12] A. Abragam, "The Principles of Nuclear Magnetism." Oxford Univ. Press (Clarendon), London and New York, 1961.

[13] S. Schramm and E. Oldfield, *Biochemistry* **22**, 2908 (1983).

$$\Delta\nu_{1/2} = \frac{1}{\pi T_2} = \frac{3\pi^2}{100}\frac{2I+3}{I^2(2I-1)}\chi^2\left(1+\frac{\eta^2}{3}\right) \times \left(3\tau_c + \frac{5\tau_c}{1+\omega_0^2\tau_c^2} + \frac{2\tau_c}{1+4\omega_0^2\tau_c^2}\right) \quad (4)$$

For nuclei with $I > 1$, Eqs. (3) and (4) are approximately accurate only when $\omega_0\tau_c \leq 1.5$.[14,15]

Above $\omega_0\tau_c \sim 1.5$, relaxations of $I > 1$ nuclei become multiexponential, with line shapes being the superposition (thus non-Lorentzian) of contributions from each exponential. Data from such species (e.g., large proteins) can be very difficult to analyze. In solids and membranes τ_c becomes even larger, and the "quadrupolar splitting" becomes a measurable and useful parameter in QNMR (see Anisotropic Motion).

Because relaxation is so intimately associated with interpretability and observability, it is often helpful to predict likely behavior using estimated τ_c, χ, and ω_0 before running difficult and potentially fruitless experiments. Table I lists typical spectral behavior for different nuclei in extreme-narrowing conditions having the same τ_c.

Exchange

Direct observation of a quadrupolar species fully bound to an enzyme is often difficult. In such cases, the only way of getting NMR information about the bound species is to observe the spectra of the free component involved in exchange with the bound species. Some strategies for extracting the needed data are discussed later in this chapter (see Selective Examples of Applications).

Anisotropic Motion

As τ_c approaches or exceeds $1/\chi$, NMR begins to detect *orientational* anisotropy and peaks broaden and eventually split. Extreme examples are found in the NMR of solids and membranes when QNMR yields multiple resonances separated by "quadrupolar splittings."[16] For liquid samples of protein–ligand complexes τ_c is usually not large enough to induce quadrupolar splitting (if $\chi = 10^5$–10^6 Hz, τ_c would have to be at least 10^{-6}–10^{-5} sec). However, true *motional* isotropy rarely exists at a local

[14] B. Halle and H. Wennerström, *J. Magn. Reson.* **44**, 89 (1981).
[15] T. Andersson, T. Drakenberg, S. Forsén, E. Thulin, and M. Swärd, *Eur. J. Biochem.* **126**, 501 (1982).
[16] C. A. Fyfe, "Solid State NMR for Chemists." CFC Press, Guelph, Ontario, Canada, 1983.

level in macromolecular systems, and the τ_c deduced from Eqs. (2)–(4) should be regarded as "effective" correlation times resulting from a combination of slower, generally isotropic overall tumbling and faster, anisotropic internal motions.

Determination of τ_c and/or χ

Correlation times and χ provide information of interest to biochemists and chemists. Because ω_0 and I are always known and η is usually negligible, relaxation times are straightforward functions of τ_c and χ according to Eqs. (2)–(4). If one of these values is known, the other can be determined from the relaxation time or linewidth using algebra (in extreme narrowing) or the Newton–Raphson (or some other) numerical method.[17]

The correlation time is strictly a motional parameter and is affected by chemistry, solvation, temperature, etc., only to the extent that these affect molecular motion. On the other hand, χ is dependent on chemical factors. When the electrical environment of the quadrupolar nuclei is defined by stable covalent bonds, χ is likely to be constant in a variety of environments provided that no change in bonding occurs. Thus, χ for a C–D species is likely to be nearly constant free and bound to an enzyme. On the other hand, χ for $^{39}K^+$ is likely to change on binding to an anion or a protein.

In ^2H NMR studies χ can be estimated by chemical analogy with similar compounds for which χ has been determined by independent techniques,[6,13,18,19] and can be used to determine changes in τ_c upon binding. In observing ligands bound to proteins, the simultaneous solution of τ_c and χ based on Eqs. (3) and (4) can be accomplished outside of extreme narrowing by measuring both T_1 and T_2 or by measuring either value at two different magnetic field strengths.

Experimental Techniques

Special Problems in QNMR

Experimental difficulties in QNMR are sometimes different from those commonly encountered in other HR NMR or solid-state NMR. In this section the nature of some of these problems is described. The discussion includes hardware and software techniques used to minimize these and other problems.

[17] R. L. Burden, J. D. Faires, and A. C. Reynolds, "Numerical Analysis," 2nd ed. Prindle, Weber, & Schmidt, Boston, 1981.
[18] P. Tsang, R. R. Vold, and R. L. Vold, *J. Magn. Reson.* **71**, 276 (1987).
[19] H. Saito, H. Mantsch, and I. C. P. Smith, *J. Am. Chem. Soc.* **95**, 8453 (1973).

Acoustic Ringing. Acoustic ringing refers to the acoustic waves generated by electromagnetic interaction of the radiofrequency pulse with probe materials. These waves result in spurious rolling in the spectral baseline and can also be manifested as a sharp spike at the beginning of a free induction decay (FID). This phenomenon is present in all NMR experiments but is typically a serious problem in QNMR. In other HR NMR, acoustic ringing can be minimized by employing a sufficiently long preacquisition delay (DE), but in QNMR the length of this DE may cause other problems (see later). Furthermore, in usual HR NMR, signals are often sharp and are easily distinguished from a rolling baseline, and the spectral width is often so small that the entire "ring" is not observed. In QNMR large spectral widths make ringing very apparent and broad peaks may be difficult to differentiate from the baseline rolling, as illustrated previously.[20,21] Acoustic ringing is also more severe at relatively low observation frequencies, a fact of some importance because many quadrupolar nuclei have low Larmor frequencies due to low magnetogyric ratios (γ). Gerothanassis recently published an excellent review[21] on the phenomenon of acoustic ringing and how to deal with it.

Need and Consequences of "Hard" Pulsing. Another consequence of the small γ possessed by many nuclei is that, under a given condition, a relatively long pulsewidth is needed. A long 90° pulse may present difficulties in complex pulse sequences and limits the breadth of spectral excitation. This latter effect is in conflict with the frequent need in QNMR to cover a large spectral range including broad signals. In order to reduce the length of the 90° pulse, higher transmitter power (to produce a "hard" pulse) must be utilized, which worsens acoustic ringing.

Preacquisition Delay (Deadtime). Many spectrometers automatically set DE equal to the dwell time to facilitate phasing. In pulsed FT NMR, the dwell time (DW) is the inverse of the sampling rate that is determined by the spectral width (SW), i.e., DW = 1/(2SW). In a typical ^{1}H NMR experiment at 300 MHz, SW = 3000 Hz and DW = 167 μsec. Because T_1 and T_2 are on the order of 0.1–10 sec (for protons), the data lost during DE are usually negligible. However, in QNMR there are a number of conflicting problems. (1) A large SW is generally needed, resulting in smaller DW (and thus a smaller default value of DE). (2) Acoustic ringing is often more serious (as described previously), which would require a longer DE to minimize. (3) T_1 and T_2 are often so short (e.g., <1 msec) that a significant portion of their signal can be lost during DE. This results in a loss of S/N,

[20] M.-D. Tsai, this series, Vol. 87, p. 235.
[21] I. P. Gerothanassis, *Prog. NMR Spectrosc.* **19**, 267 (1987).

distortion of peaks,[22] and problems in intensity/integration measurement. As a result, the T_1 data should be treated with caution, and the integrated signals with different linewidths cannot be compared.

Hardware Considerations

Magnet and Console. Large superconducting magnets have the advantages of superior sensitivity and stability and result in higher Larmor frequencies. However, because of the broad signals usually encountered in QNMR, resolution and field stability requirements are often less stringent than in typical HR work.

Rapid pulsing and data sampling of a great number of scans require a high dynamic range, which puts high demands on the electronic and computational components of the spectrometer system.

The Probe. The performance of the probe is a key variable in QNMR. In QNMR, as for solid-state NMR, high-power probes are frequently used.[21,22] These probes generally utilize a single horizontal solenoid transmitter/receiver coil which is inherently more sensitive than Helmholtz saddle coils. These coils produce a short 90° pulse compared to saddle coils and also handle higher pulse power more efficiently. High-power probes are also built with materials chosen to reduce acoustic ringing (a negative factor in terms of sensitivity).

The disadvantages of high-power probes lie in the difficulty of shimming and achieving high resolution. Furthermore, they often possess no locking or spinning capability. Fortunately, these factors are usually less important in QNMR. Sample change is also laborious because the entire probe has to be removed from the magnet.

High-resolution probes are often quite suitable when linewidths are not too broad, and these probes are a necessity when accurate linewidths are needed in the high-resolution region.

Software Considerations

Pulse Sequences. When initiating a study, a standard single-pulse experiment can be attempted to evaluate the system at hand (sensitivity, baseline distortion, linewidth, etc.). At this point, DE could be manually adjusted to either reduce acoustic ringing (larger DE) or to increase S/N (smaller DE).[20] Alternatively, one can employ a pulse sequence which will reduce acoustic ringing. Many such pulse sequences have recently become available and have been reviewed by Gerothanassis.[21] In our

[22] E. Fukushima and S. B. W. Roeder, "Experimental Pulse NMR—A Nuts and Bolts Approach," Addison-Wesley, Reading, Massachusetts, 1981.

experience the RIDE (ring-down elimination) sequence[4,21,23] worked effectively.

Some pulse sequences involving use of spin echoes have also been developed for QNMR.[21] When T_2 is very short but T_1 is much longer, spin-echo techniques should allow the true spectra to be observed and also can increase S/N.[21,24,25] However, when T_1 and T_2 are both very short (0–100 μsec), acquisition becomes very difficult due (among other reasons) to the significant relaxation that occurs during the actual pulse sequence. To our knowledge, there is no way around this problem in pulsed FT NMR and in this case CW NMR can actually be advantageous if sensitivity is not a big problem.[21,26] (CW NMR also eliminates the problems associated with generating adequate pulse power to cover a very broad spectral width.)

Although the sampling rate could be as high as 100 scans per sec, it should be kept in mind that the recycling time needs to be $\geq 3T_2$ to avoid truncation of the FID (which will cause a regular series of spikes at the bottom of the peak),[27] and needs to be $\geq 5T_2$ when the quantitative intensity is of interest.[28] Becker *et al.*[29] presented a lucid description of the optimization of pulse repetition times as well as pulse angles.

T_1/T_2 Determination. The relative merits of the various T_1/T_2 determination methods have been discussed extensively.[26] These methods can be integrated into the sequences used to minimize acoustic ringing. Data taken for very short T_1/T_2 should be interpreted with caution, because these data may deviate from true values due to significant relaxation during pulsing and DE.

Selective Examples of Applications

Metal Ion Binding to Proteins

As shown in Table I, many biologically relevant metal ions are quadrupolar nuclei. QNMR has been extensively utilized to study binding of these ions to various proteins, as described by several reviews.[2,3,23,30] The

[23] H. J. Vogel and S. Forsén, *Biol. Magn. Reson.* **7**, 247 (1986).
[24] A. Allerhand and D. W. Cochran, *J. Am. Chem. Soc.* **92**, 4482 (1970).
[25] E. D. Becker, J. A. Ferretti, and T. C. Ferrar, *J. Am. Chem. Soc.* **91**, 7784 (1969).
[26] M. Llinas and A. DeMarco, *J. Am. Chem. Soc.* **102**, 2226 (1980).
[27] A. E. Derome, "Modern NMR Techniques for Chemical Research," Vol. 6 of the Organic Chemistry Series. Pergamon, Oxford, 1987.
[28] M. L. Martin, J.-J. Delpuech, and G. J. Martin, "Practical NMR Spectroscopy." Heyden, London, 1980.
[29] E. D. Becker, J. A. Ferretti, and P. N. Gambhir, *Anal. Chem.* **51**, 1413 (1979).
[30] W. H. Braunlin, T. Drakenberg, and S. Forsén, *Curr. Top. Bioenerg.* **14**, 97 (1985).

most successful study in this category is binding of Ca^{2+} to calmodulin (CaM), which is used to illustrate the procedures, problems, and interpretations of the actual experiments.

CaM (M_r 16,800) has four Ca^{2+}-binding sites, numbered I–IV starting from the N-terminus. Various studies have suggested that the four sites can be grouped into two high-affinity sites (III and IV, $K_a \approx 10^6$–$10^7\ M^{-1}$) and two lower affinity sites (I and II, $K_a \approx 10^5$–$10^6\ M^{-1}$).[31-34] The ^{45}Ca NMR signals of Ca^{2+} fully bound to the high-affinity sites have been observed at 2.8 mM CaM and 4.8 mM Ca^{2+}, with $\Delta\nu_{1/2} = 770 \pm 50$ Hz ($T_2 = 0.42$ msec). An inversion–recovery experiment determined $T_1 = 0.86$ msec. The nonequivalence of T_1 and T_2 suggests that the system is not in the extreme narrowing limit and Eq. (2) cannot be applied. Because CaM is a small protein and satisfies $\omega_0\tau_c \leq 1.5$, even if binding is totally rigid, Eqs. (3) and (4) can be used to solve for χ (1.1 MHz) and τ_c (8.2 nsec) simultaneously from T_1 and T_2.[15]

Additional information concerning binding of Ca^{2+} and Mg^{2+} to CaM have been obtained by titration and temperature-dependence experiments, which are illustrated using ^{25}Mg NMR.[35] Because the affinity of Mg^{2+} to CaM is much weaker than that of Ca^{2+}, it is not possible to observe fully bound Mg^{2+}. Even if a large excess of CaM can be used to fully bind Mg^{2+}, the larger quadrupole moment of Mg^{2-} could result in a $\Delta\nu_{1/2}$ too large to be measured at the concentration used. Figure 1 shows ^{25}Mg NMR spectra at different ratios of $CaM \cdot Ca_2^{2+}$ (which represents CaM when sites III and IV are saturated with Ca^{2+} and sites I and II are open for binding Mg^{2+}). The plots of $\Delta\nu_{1/2}$ versus $[Mg^{2-}]/[CaM \cdot Ca_2^{2+}]$ are shown in Fig. 2A. All spectra are Lorentzian, as exemplified in spectra I and J (fittings of A and H, respectively). The Lorentzian shape and the successive changes in linewidths rule out the possibility that the observed signal is due to overlap of the signals of free and bound Mg^{2+} in *very slow exchange* relative to the NMR time scale (Case A in Table II). There are, however, three other possible interpretations. (1) The observed signal is due to free Mg^{2+}, which is in *slow exchange* with bound Mg^{2+} [Case B(a) in Table II]. The signal of bound Mg^{2+} is either too broad to be detected or is well separated from the observed signal of free Mg^{2-} so that the signal

[31] J. D. Potter, P. Strang-Brown, P. L. Walker, and S. Iida, this series, Vol. 102, p. 135.
[32] J. A. Cox, M. Comte, A. Malone, D. Burger, and E. A. Stein, *Metal Ions Biol. Syst.* **17**, 215 (1984).
[33] S. Forsén, H. J. Vogel, and T. Drakenberg, *in* "Calcium and Cell Function" (W. Y. Cheung, ed.), Vol. 6, pp. 113–157. Academic Press, New York, 1986.
[34] C.-L. A. Wang, *Biochem. Biophys. Res. Commun.* **130**, 426 (1985).
[35] M.-D. Tsai, T. Drakenberg, E. Thulin, and S. Forsén, *Biochemistry* **26**, 3635 (1987).

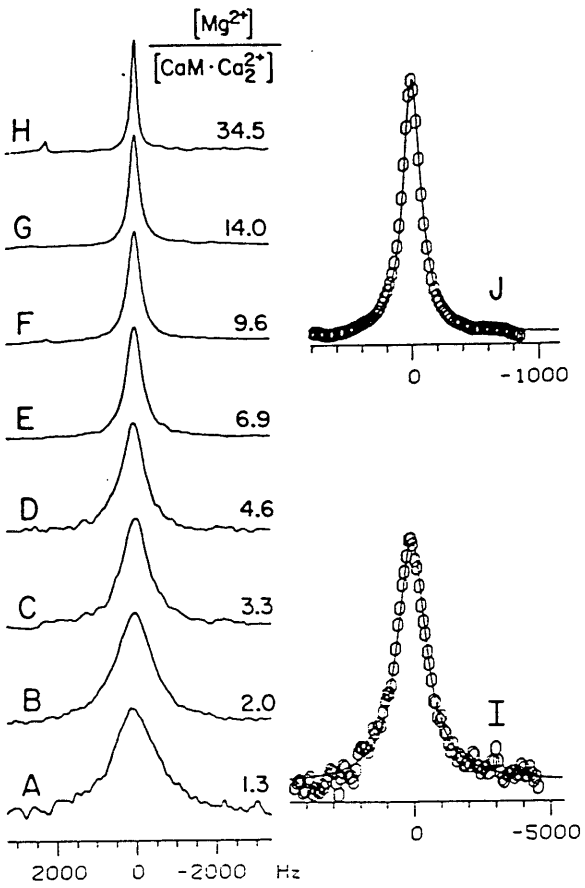

FIG. 1. ^{25}Mg NMR spectra (at 22.15 MHz, 25°) of Mg^{2+} at various ratios of $[Mg^{2+}]/[CaM \cdot Ca_2^{2+}]$ (A–H). Spectra I and J are the Lorentzian fits of spectra A and H, respectively. The circles in spectra I and J represent experimental data, and the solid lines represent the fitted spectra. The RIDE sequence was used to reduce acoustic ringing. The line broadening used is 100 Hz. (Reproduced from Tsai *et al.*[35] with permission.)

remains Lorentzian. The broadening is caused by chemical exchange as shown in Table II. (2) The observed signal is due to the *fast exchange* average of free and bound Mg^{2+} [Case C(a) in Table II] and the successive broadening is mainly due to the rapid relaxation (large $\Delta\nu_{1/2}$) of bound Mg^{2+}. (3) The system is in the *intermediate exchange* region (Case D in Table II), and the broadening is caused by chemical exchange and by averaging with bound Mg^{2+}.

A temperature-dependence study can differentiate the above situa-

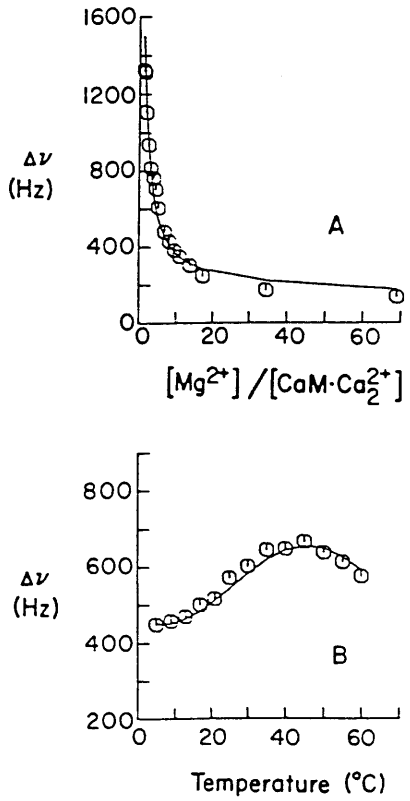

FIG. 2. Titration curve (A) and temperature curve (B) of Mg^{2+} binding to $CaM \cdot Ca_2^{2+}$. The titration curve was obtained at 25°. The temperature curve was obtained at $[Mg^{2+}]/[CaM \cdot Ca_2^{2+}] = 5.24$. Circles are experimental points and solid curves are obtained by connecting the calculated points from the iterative fitting. The $\Delta\nu$ values shown include a line broadening of 100 Hz. (Reproduced from Tsai *et al.*[35] with permission.)

tions. In the case of slow exchange, increasing temperature will increase the exchange rate (i.e., increase $1/\tau_{ex}$) and cause an increase in the observed $\Delta\nu$ if the increase due to exchange rate is large enough to outweigh the decrease in the intrinsic linewidth (due to increased molecular motion). In the case of fast exchange, the intrinsic linewidths of both free and bound Mg^{2+} decrease due to decreasing τ_c, which will result in a decrease in the observed $\Delta\nu_{1/2}$ upon increasing temperature. Figure 2B shows that the $Mg^{2+}/CaM \cdot Ca_2^{2+}$ system is in slow exchange at 25° and gets into the intermediate region at 30–50°.

When such a complete set of data can be obtained, the data can be analyzed by "total line shape analysis." The details of such analysis have

TABLE II
EFFECTS OF EXCHANGE ON TITRATION EXPERIMENTS AND TEMPERATURE DEPENDENCE OF $\Delta\nu_{1/2}$[a]

Cases	Titration experiments	Temperature dependence
A. Very slow exchange $\frac{1}{\tau_{ex}} \ll \frac{1}{(T_{1,2})_b}$	(a) Bound species not detectable: one Lorentzian signal with successive decrease in intensity, but with constant $\Delta\nu_{1/2}$	$\Delta\nu_{1/2}$ decreases with increasing temperature due to decreasing τ_c
	(b) Bound species detectable: two signals, or one apparently non-Lorentzian signal, if the two signals overlap	
B. Slow exchange $\frac{1}{\tau_{ex}} < \frac{1}{(T_{1,2})_b}$	(a) Bound species not detectable: one Lorentzian signal, successively broadened $\frac{1}{T_{1,2}} = \frac{1}{(T_{1,2})_f} + \frac{1}{\tau_{ex}}\frac{P_b}{P_f}$ (6) or $\Delta\nu_{1/2} = \Delta\nu_f + \frac{1}{\pi\tau_{ex}}\frac{P_b}{P_f}$	$\Delta\nu_{1/2}$ increases with increasing temperature due to decreasing τ_{ex}
	(b) Bound species detectable: two signals, each broadened by exchange, or one apparently non-Lorentzian signal, if the two signals overlap	
C. Fast exchange $\frac{1}{\tau_{ex}} \gg \frac{1}{(T_{1,2})_b}$	(a) Exchange narrowing ($1/\tau_{ex} \gg \Delta\omega$): one signal. $\frac{1}{T_{1,2}} = \frac{P_f}{(T_{1,2})_f} + \frac{P_b}{(T_{1,2})_b}$ (7)	Same as A
	(b) Not exchange narrowing ($1/\tau_{ex} \ll \Delta\omega$): two signals separated by $\Delta\omega$	
D. Intermediate exchange $\frac{1}{\tau_{ex}} \sim \frac{1}{(T_{1,2})_b}$	In between B and C	Irregular or insensitive

[a] $1/\tau_{ex}$ is the ligand–protein on/off exchange rate (k_{ex}), b and f designate free and bound states, respectively, $\Delta\omega$ represents the separation in resonance frequencies of free and bound ligands, and P_f and P_b represent fractions of ligand in free and bound states, respectively. Only one ligand site per molecule is assumed as is the relationship $1/(T_{1,2})_b \approx 1/(T_{1,2})_b - 1/(T_{1,2})_f$.

been described elsewhere[36] and are beyond the scope of this article. The curves in Fig. 2 resulted from iterative fittings, which yielded the following information: $K_a = 2000\ M^{-1}$ (assuming two equivalent sites), k_{off} ($\approx k_{ex}$) = 2300 sec^{-1}, and $\Delta\nu_{1/2}$ = 3.5 kHz for bound Mg^{2+}. In this case, τ_c and χ cannot be obtained simultaneously, but if τ_c of Mg^{2+} is assumed to be the same as τ_c of Ca^{2+} when bound to CaM, χ = 1.6 MHz can be obtained. The result unequivocally establishes that Mg^{2+} binds to sites III and IV of CaM, as described in detail by Tsai *et al.*[35]

In many other studies, complete line shape analysis by the above method is not possible because the complete temperature range may not be obtainable, and the protein available for experiments may be limited in quantity and stability. Even if the protein is stable enough for a variable temperature study, the system may remain in slow (or fast) exchange throughout the entire region. The titration data of these systems are frequently analyzed by the "Swift–Connick" equation[37] [Eq. (5)], which is a combination of Eqs. (6) and (7) described in Table II when $P_f \approx 1$ and $P_b \ll 1$:

$$\frac{1}{T_{1,2}} = \frac{1}{(T_{1,2})_f} + \frac{P_b}{\tau_{ex} + (T_{1,2})_b} \tag{5}$$

Equation (5) is applicable for slow, intermediate, and fast exchange regions. It allows a straightforward measurement of $1/(\tau_{ex} + T_{2_b})$ from the slope of the plot of $(\pi\Delta\nu_{1/2})$ versus P_b. Because $P_b \ll 1$ (e.g., 0–5%), it can often be assumed that P_b = [protein]/[ligand]$_{total}$. The main problem in this approach is to determine whether the system is in slow exchange (slope = $1/\tau_{ex}$ because $\tau_{ex} \gg T_{2_b}$), fast exchange (slope $\approx \pi\Delta\nu_b$ because $T_{2_b} \gg \tau_{ex}$), or intermediate exchange (slope is not directly interpretable).

Halide Ion Binding to Proteins

The technical problems for halide ion binding are very similar to those of metal ion binding to proteins, but the systems amenable to such studies are more limited. Well-studied proteins include, among others, hemoglobin[38] and Cl^- transport proteins.[39,40] One advantage of ^{35}Cl NMR is that fast exchange can be established by the following criterion[3]:

[36] T. Drakenberg, S. Forsén, and H. Lilja, *J. Magn. Reson.* **53**, 412 (1983).
[37] T. J. Swift and R. E. Connick, *J. Chem. Phys.* **37**, 307 (1962).
[38] E. Chiancone, J.-E. Norne, and S. Forsén, this series, Vol. 76, p. 552.
[39] J. J. Falke and S. I. Chan, *J. Biol. Chem.* **260**, 9537 (1985).
[40] J. J. Falke, K. J. Kanes, and S. I. Chan, *J. Biol. Chem.* **260**, 9544 (1985).

$$\frac{(\Delta\nu - \Delta\nu_f) \quad \text{for} \quad {}^{35}\text{Cl}}{(\Delta\nu - \Delta\nu_f) \quad \text{for} \quad {}^{37}\text{Cl}} = \left(\frac{\chi \quad \text{for} \quad {}^{35}\text{Cl}}{\chi \quad \text{for} \quad {}^{37}\text{Cl}}\right)^2 = 1.60 \tag{8}$$

where $\Delta\nu$ and $\Delta\nu_f$ represent the observed linewidth and the linewidth of free Cl^-, respectively. In Cl^- binding studies, fast exchange is observed in most cases, and the detailed ^{35}Cl NMR analysis under various conditions (e.g., pH dependence and effect of other ligands) has been used to deduce the number and the environment of Cl^- binding sites.

Substrate Binding to Enzymes

The most desirable information in this category is the "internal motions of bound substrates." It is widely accepted that enzyme-bound substrates possess a certain extent of internal rotational freedom relative to the enzyme. However, it is difficult to describe the dynamics of bound substrates quantitatively, because a single measurement can yield only the *effective* τ_c, which may include contributions from several motional components. Indeed, more studies have been done on the dynamics of local segments of proteins (e.g., London [18] and Keniry [19], Vol. 176, this series) than that of bound substrates. The latter studies are often complicated by exchange processes as described previously herein.

In enzyme–substrate binding studies, ^2H NMR has been used to show that the adenine portion of NAD^+ bound to lactate dehydrogenase has a longer τ_c than the τ_c of the pyridine ring,[41] and that when linoleic acid is bound to lipoxygenase, the internal motions of the substrate increase at positions away from the carboxylic acid group.[42] We describe in detail a binding study of adenylate kinase (AK) using ^2H NMR.[43]

Chicken muscle AK was titrated with adenylyl(β,γ-methylene) diphosphonate (AMPPCP) deuterated on the phosphonate chain and on the adenine ring and followed by measuring the ^2H NMR linewidth of the single peak that results from the average of the bound and free AMPPCP. Plots of $\Delta\nu_{1/2}$ versus $[\text{AMPPCP}]_{\text{bound}}/[\text{AMPPCP}]_{\text{total}}$ were linear, as shown in Fig. 3. The line shapes of the observed peaks were usually Lorentzian, and limited T_1 inversion recovery data taken were always monoexponential. Thus, the data meet "fast-exchange" criteria and the linewidths of the fully bound species can be determined from linear extrapolations to the fraction bound equal to 1.[44] The effective τ_c values were then calcu-

[41] A. P. Zens, P. T. Fogle, T. A. Bryson, R. B. Dunlap, R. R. Fisher, and P. D. Ellis, *J. Am. Chem. Soc.* **98**, 3760 (1976).
[42] T. S. Viswanathan and R. J. Cushley, *J. Biol. Chem.* **256**, 7155 (1981).
[43] C. R. Sanders II and M.-D. Tsai, *J. Am. Chem. Soc.* **110**, 3323 (1988).
[44] A. C. McLaughlin and J. S. Leigh, *J. Magn. Reson.* **9**, 296 (1973).

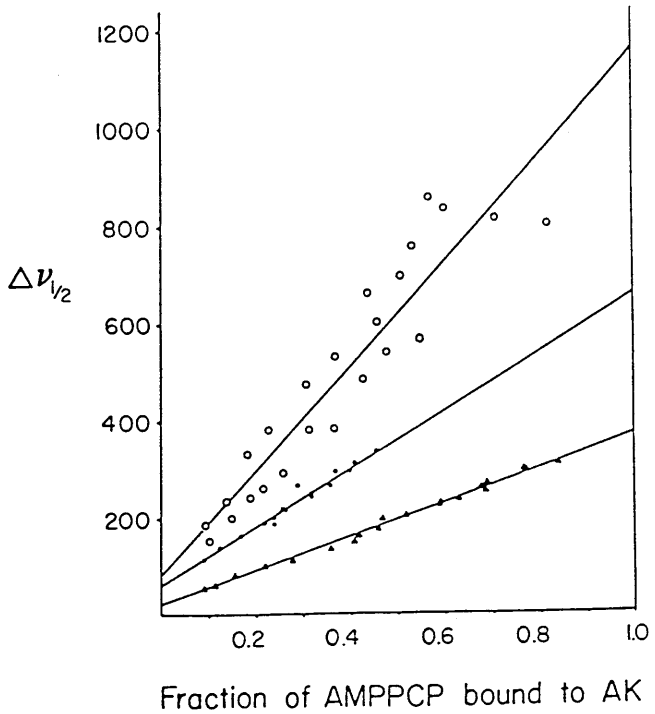

FIG. 3. High-resolution ^2H NMR (46.1 MHz) linewidths ($\Delta\nu_{1/2}$ in hertz) of ^2H-labeled AMPPCP and MgAMPPCP as a function of fractions bound to AK. The experiments were carried out by titrating 1–2 m*M* AK with small aliquots of AMPPCP or MgAMPPCP ($[Mg^{2+}]/[AMPPCP] = 4$). Sample conditions: pH 7.0 in ^2H-depleted H_2O with 45 m*M* HEPES–K^+ or imidazole–HCl, 117 m*M* KCl, 1–8 m*M* dithiothreitol, and 0.1 m*M* EDTA in a 10-mm NMR tube (starting volume of 1.75 ml). Spectral conditions: the probe temperature was 10°; the digital resolution varied from 1 Hz/point for narrow signals to 15 Hz/point for very broad signals; the 90° pulsewidth was 12 μsec. The CYCLOPS pulse sequence was used. The reported $\Delta\nu_{1/2}$ have been corrected for line broadening (1–10 Hz). The fraction of AMPPCP bound to AK was calculated using K_d values of 210 μ*M* for AMPPCP and 190 μ*M* for MgAMPPCP. (○) [8-^2H]AMPPCP, (●) MgAMPPCD$_2$P, and (▲) AMPPCD$_2$P. (From Sanders and Tsai.[43])

lated from Eq. (4) using values of χ from structurally related compounds. The contributions of two-bond ^2H–^{14}N and ^2H–^{31}P scalar and dipolar couplings to the observed $\Delta\nu_{1/2}$ were insignificant. The validity of deducing τ_c from linewidths was further supported by limited T_1 experiments.

The τ_c values obtained indicate that the adenine ring of bound AMPPCP is motionally rigid (τ_c = 27 nsec) and approaches the overall τ_c of AK. The β–γ region of the phosphonate chain (τ_c = 7 nsec) possesses considerable local mobility, consistent with more qualitative ^{17}O NMR

studies.[45] This motional freedom is reduced upon binding of Mg^{2+} (τ_c = 16 nsec). The implication of these dynamic properties on the catalytic mechanisms of AK has been discussed.[43]

[45] D. A. Wisner, C. A. Steginsky, Y.-J. Shyy, and M.-D. Tsai, *J. Am. Chem. Soc.* **107,** 2814 (1985).